Applied Acoustics 71 (2010) 45–51

Contents lists available at ScienceDirect

Applied Acoustics

journal homepage: www.elsevier.com/locate/apacoust

Low-frequency sound wave parameter measurement in gravels

George W. Swenson Jr. [a,*], Michael J. White [b], Michael L. Oelze [a]

[a] Department of Electrical and Computer Engineering, University of Illinois at Urbana-Champaign, 1308 West Main Street, Urbana, IL 61801, United States
[b] US Army Engineer Research and Development Center, Construction Engineering Research Laboratory, P.O. Box 9005, Champaign, IL 61826, United States

ARTICLE INFO

Article history:
Received 16 October 2008
Received in revised form 9 July 2009
Accepted 14 July 2009
Available online 12 August 2009

Keywords:
Attenuation
Phase velocity
Wavelength
Porous media
Granular media
Impedance tube
Gravel

ABSTRACT

Experiments were performed to measure the various sound-wave propagation parameters of two kinds of gravel, a crushed limestone and a stream-formed "pea gravel", at frequencies between 25 and 200 Hz. The apparatus was a very large standing-wave tube with an array of microphones along its entire length. Measurements were made with the tube in the vertical position, filled to various depths, with a pressure-doubling barrier at the bottom. Values were determined for wavelength and attenuation in the gravel and for input impedance at the boundary between gravel and air. The basic analysis method was to fit the parameters of a presumed Green's function representing the standing wave in the tube to the measured sound pressure amplitudes measured by the microphones. This worked well for some frequencies and some depths of gravel. In other cases, various modifications of the method gave more consistent results. For crushed limestone, the estimates of phase velocity and attenuation increased monotonically with frequency, ranging between 150 and 250 m/s and 0.1 and 0.8 Np/m, respectively. For pea gravel, the estimates increased monotonically with frequency, with values between 160 and 205 m/s and 0.4 and 1.1 Np/m, respectively.

1. Introduction

This document reports the experimental results of a study of low-frequency (25–200 Hz) sound-wave propagation in two representative types of "gravel": a coarse crushed limestone and a smaller, stream-formed "pea gravel". Such materials have been considered as media for the absorption of sound energy from military activities such as demolition and artillery training, and there is a paucity of available information on their sound absorption and propagation properties at the low frequencies characteristic of the noise of such activities. While theories exist for sound waves in porous media [1], very few have been tested for the prediction of propagation or absorption effects in the low-frequency range under consideration [2–4]. Thus there exists a need for basic experimental data that can be used for the prediction of sound absorption and propagation in various contexts.

Several experiments have reported acoustic characteristics of rigid, air-filled porous media. Papers reporting measurements of dispersion, attenuation and impedance for gravel, sand, or soils include Attenborough [5], Bolen and Bass [6], Dickinson and Doak [7], Embleton et al. [8], Frederickson et al. [3], Hess et al. [9], Hickey and Sabatier [10], Hutchinson-Howorth et al. [11], Song and Bolton [12], Oelze et al. [13], and Lu et al. [14]. Of those papers, only three report data for frequencies as low as 100 Hz, and only Bolen and Bass [6] report data for 40 Hz. The level-difference technique used by Hess et al. [9], and the propagation inverse-modeling approach of Bolen and Bass [6], Dickinson and Doak [7], and Embleton et al. [8] become insensitive to the value of ground impedance for low frequencies such as 40 Hz and 100 Hz. The impedance tube first used by Dickinson and Doak [7] is difficult to manage for outdoor measurements, and requires lengths comparable to one-quarter wavelength in air for the lowest frequency of interest.

Sound propagation experiments within and over porous media present many difficulties; for example, from the susceptibility of buried microphones to damage from the porous medium, from mathematical complications arising from three-dimensional geometry, and from the lack of structural rigidity of many porous materials. Therefore, an experimental procedure was developed to acquire acoustic wave propagation data at low frequency, which could avoid the above-mentioned difficulties.

2. Description of facilities

The US Army Engineer Research and Development Center, Construction Engineering Research Laboratory (ERDC/CERL) has a suite of acoustical impedance-measuring facilities intended for use at low frequencies [15,16]. One of the instruments is a Kundt's tube (or "Impedance Tube"), consisting of a 7.3-m long, 76-cm diameter Schedule 80 steel pipe, with microphone ports every 20 cm along a straight line in the wall of the tube (see Figs. 1 and 2). There is 30 cm of separation between the loudspeaker face and the topmost

* Corresponding author. Tel.: +1 217 352 6511.
E-mail address: gswenson@illinois.edu (G.W. Swenson Jr.).

0003-682X/$ - see front matter © 2009 Elsevier Ltd. All rights reserved.
doi:10.1016/j.apacoust.2009.07.003

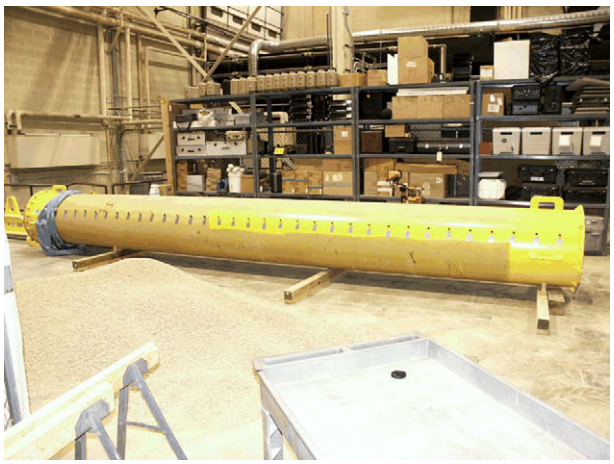

Fig. 1. Impedance tube in the horizontal position, showing the microphone ports. Photo by Timothy Onder.

Fig. 2. Impedance tube in the vertical position. Microphones not installed. Photo by Timothy Onder.

microphone. The lowest microphone is 21 cm above the terminating plate. Schedule 80 pipe in this size has a wall thickness of 12.7 mm. A heavy steel lid is bolted to one end of the tube, presumably forming a rigid termination, and a 12-in loudspeaker (MTX Thunder T9512-04) in a heavy plywood baffle forms the driving source at the other end. Instantaneous sound pressures are measured by 32 precision microphones in the ports and voltages corresponding to the instantaneous sound pressures are recorded by two 16-channel oscilloscopes (Yokogawa DL750 ScopeCorder). The loudspeaker can be excited by continuous-wave signals at discrete frequencies or by broad-band random noise. A variety of laboratory-grade instrumentation microphones in one-inch and half-inch sizes (Bruel and Kjaer and Larson-Davis) were used in different combinations for different data-collecting runs. Before each run, all microphones were calibrated by a Bruel and Kjaer type 4228 pistonphone at 250 Hz. No differences have been observed in the performance of any of the microphones.

For experimental investigation of the properties of the porous medium, gravel in this case, the tube is filled part way, leaving a substantial depth of air above the gravel. It is assumed that the porous medium is homogeneous and isotropic on a length scale of a small fraction of a wavelength, and that the sound field can be modeled by the classical wave equation. The radial dimension of the tube is expected to restrict the sound field to plane-wave modes along the length of the pipe at the frequencies of interest, and the rigid barrier at the bottom of the tube is assumed to be a pressure-doubling surface. The wave propagation parameters required to fully characterize the acoustic properties of the porous medium are attenuation, phase velocity, complex intrinsic impedance and complex input impedance at the air/medium boundary. The phase velocity and the wavelength at a given frequency can, of course, be determined from one another. Also, the complex input impedance is completely dependent on the other propagation parameters. The wave propagation parameters can, in principle, be determined by choosing a Green's function that represents both incident and reflected pressure waves in both the filled and unfilled portions of the tube, and fitting the unknown parameters of the Green's function to the measured data by a least mean-squares estimation (LMSE) procedure. With 32 measured sound pressure values available it should be possible to determine the few unknown parameters (two real-valued parameters, i.e., the phase velocity and attenuation, and one complex-valued parameter, i.e., the reflection coefficient). The parameters of the air above the filled portion of the tube are presumed to be known.

In practice, the process does not work equally well for all parameters and for all frequencies and both types of gravel, and it has proven necessary to use a number of special procedures for the determination of some of the combinations. These procedures are described below and in more detail in [17]. In the case of the intrinsic impedance, no credible determinations have so far been achieved, though all other parameters can be reported with a satisfactory degree of confidence.

All measurements were taken in the impedance tube terminated with a heavy steel plate, massively stiffened, underlying a gravel layer of variable depth L. At the upper end of the impedance tube a loudspeaker was used to generate either a tone or band-limited random noise. The source frequency was kept low in order to propagate only plane waves normally incident upon the interfaces of air/gravel and gravel/steel plate. The transverse modes comprising the field around the loudspeaker are evanescent and strongly decaying. The x-axis has its origin at the gravel-backing interface (i.e., gravel/steel plate), and x is increasing upward (see Fig. 3). For the fields below the speaker region within medium 0 ($x \geqslant L$,

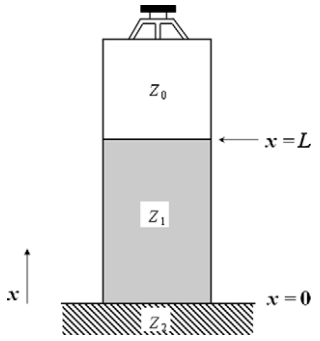

Fig. 3. Schematic geometry of the experimental setup.

air), medium 1 ($L \geqslant x \geqslant 0$, gravel) and at the bounding medium 2 ($x = 0$, rigid), the spectral sound pressure is

$$P(x,f) = \begin{cases} A_0[e^{j\beta_0(x-L)} + \Gamma_{01}e^{-j\beta_0(x-L)}], & x \geqslant L \quad \text{(air)} \\ A_1[e^{j(\beta_1 - j\alpha_1)x} + e^{-j(\beta_1 - j\alpha_1)x}], & L \geqslant x \geqslant 0 \quad \text{(porous)} \end{cases} \tag{1}$$

where $\Gamma_{01}(f)$ is the reflection coefficient and $\alpha(f)$, $\beta(f)$ are the attenuation and phase parameters, respectively. All of the above parameters depend on frequency f. As given, Eq. (1) describes a complex-valued spectral sound pressure, composed of incident (downgoing) and reflected (upgoing) waves, where A_0 has the magnitude and phase of the source. By fitting the measured rms sound pressure to $|P|$ of Eq. (1) through a LMSE process, estimates of acoustic propagation parameters, i.e., wavelength and attenuation, can be obtained.

The impedance Z_2 for the hard backing is assumed to be infinite, so the sound pressure is twice the incident value at the backing plate ($x = 0$). At the 01 interface ($x = L$), the sound pressure solutions on either side must match in value, and the same condition applies to the particle velocity, yielding

$$A_0(1 + \Gamma_{01}) = 2A_1 \cos[(\beta_1 - j\alpha_1)L] \tag{2}$$

These relations complete the specification of the spectral sound pressure within and above the porous layer.

3. Estimation of parameters

The rms sound pressures measured along the impedance tube vary with position, and the shapes of the standing wave profiles relate the propagation features involved. The shape of the standing wave profile (rms sound pressure vs. height) varies distinctively in response to depth of material, wavelength within the air, and within the material, and attenuation coefficient within the material. With sufficient data it should, in principle, be possible to estimate the few unknown wave parameters by a combined LMSE fit [18] of the Green's function, Eqs. (1) and (2), to the measured sound pressure data. The fitting process seeks to minimize a residual error, chosen here as the mean of the squared differences between the measured rms sound pressures and the evaluation of $|P|$, at microphone positions x_i,

$$\delta^2 = N^{-1}\sum_{i=1}^{N}[P_{\text{meas, rms}}(x_i) - |P(x_i)|]^2 \tag{3}$$

When evaluating δ^2 of Eq. (3), a combination of values was chosen for the unknown parameters (α_1, β_1, Γ_{01}, and A_0), alongside a set of known values for parameters β_0 and L, all needed to completely specify $P(x)$ of Eq. (1). Under LMSE fitting, the unknown parameters were adjusted in combination, δ^2 was evaluated, and the combination was reported that minimized δ^2. When generating trial combinations, each parameter was assigned a plausible range and step size over which it was varied. For example, the attenuation coefficient was initially restricted to the range, $0 \leqslant \alpha_1 \leqslant 10$ Np/m, with 101 steps spanning the range. The real and imaginary parts of Γ_{01} and A_0 were each treated as independent parameters with separately assigned ranges.

The LMSE adjustment of the parameters of the combined Green's function, Eq. (1), to the measured sound pressure amplitudes was performed using signals at the discrete frequencies 25, 50, 75, 100, 150 and 200 Hz. An example data set and fit is shown in Fig. 4. As mentioned above, with pressure amplitude data available at 32 points along the impedance tube, and with the known wave number in the air-filled portion of the tube, this proved to be difficult for some frequencies and some parameters. So, it was necessary in some cases to introduce analysis techniques tailored to specific parameters.

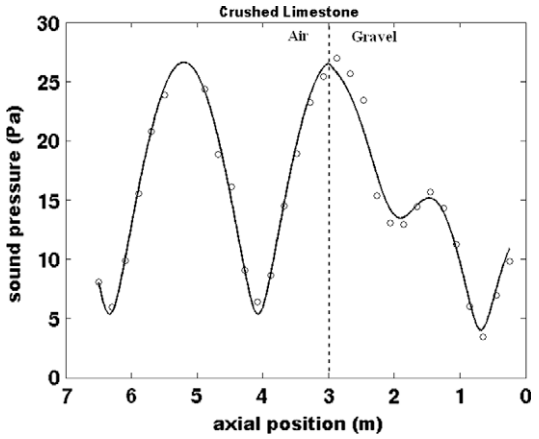

Fig. 4. Typical data set, rms sound pressure amplitudes: 75 Hz, 3.0 m of gravel. Attenuated standing wave is evident in the porous medium.

When the LMSE procedure does not converge to credible values of attenuation or phase velocity/wavelength, or when separate determinations are desired for reasons of confidence, more direct analysis techniques can sometimes be used. For example, phase velocity can be estimated from the time correlation of pressure signals between separated microphone ports; this appears to work best with band-limited random noise signals. The time delay for maximum correlation, divided into the linear distance between sampling points, yields the phase velocity. At frequencies for which the attenuation is high or at which multiple cycles of the standing wave exist in the porous medium, the exponent of a real exponential function can be fitted to the measured pressure data to determine the attenuation term of the complex wave number. Fitting to an exponential in this way amounts to replacing Eq. (1) by the expression $P(x) \approx A_1 \exp(\alpha_1 x)$ and neglecting the (presumed) smaller effects of the interference pattern. Both these latter methods agree well with results of the more general LMSE procedure at those frequencies at which both techniques are useful. While this paper represents a concise but sufficiently extensive presentation of the experimental measurements and data analysis procedures, additional details of the experiments and data analysis procedures are available elsewhere [17,19,20].

4. Results

The wave propagation parameters were estimated for two types of gravel: crushed limestone and pea gravel. The discussion in this section refers to five methods of estimating these parameters. The first, called the *exponential fit*, adjusts a single exponential $A_1 \exp(\alpha_1 x)$ to the pressure standing wave entirely within the porous medium to obtain α_1. The second method, the *porous medium fit*, considers only the standing wave in the porous medium and applies Eq. (1) for $L \geqslant x \geqslant 0$. The obtained quantities are α_1, β_1, λ_1 and c_1. The third method, the *air layer fit*, applies Eq. (1) within the region $x \geqslant L$ to obtain Γ_{01} and Z_{01}. The fourth method, the *combined fit*, applies Eq. (1) in both the porous layer and in the air, subject to the boundary condition of Eq. (2). In the combined fit the obtained quantities include $\alpha_1, \beta_1, \lambda_1, c_1, \Gamma_{01}$, and Z_{01}. Finally, the *correlation method* refers to obtaining results for phase velocity c_1, and thus wavelength λ_1, via the cross correlation maximum as mentioned above.

4.1. Crushed limestone

We tested Type CA-7 crushed limestone which is graded as follows: all particles are less than 25 mm in size, 50% are less than 12.5 mm, 7.5% less than 6.3 mm and 2% less than 1.8 mm.

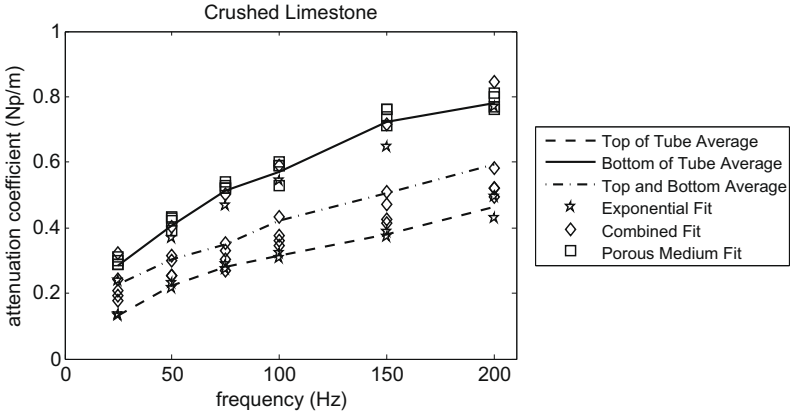

Fig. 5. Attenuation coefficient in different segments of the impedance tube estimated by the exponential fit, combined fit, and porous medium fit. Estimates using mostly ports above the middle of the filled tube show an average attenuation that is about half that of estimates using ports primarily below the middle. For estimates using nearly equal numbers of ports above and below the middle of the tube, the average values lay between the other two. Symbols closest to the lines corresponding to the top or bottom of the tubes represent estimates from the top or bottom of the tube.

Fig. 5 shows the results for the attenuation in nepers/m as a function of frequency measured by two methods at different depths of crushed limestone. Values were obtained by the exponential fit method by using amplitude data from the top half of the tube when it was filled to 7-m depth. In this circumstance the reflected wave at the top half has been substantially attenuated so that the standing wave ratio is small; furthermore, at the four higher frequencies the porous medium fit to the data exhibits only small departures above and below the exponential component and these positive and negative departures tend to cancel each other in the exponential fitting process (see Fig. 4). A plot of attenuation vs. frequency is given in Fig. 5. At the two lower frequencies the standing wave ratio is much higher owing to the lower attenuation and significant reflected wave from the steel plate. Also, the wavelength is longer so the excursions from the exponential curve do not balance out. Thus, the porous medium fit is preferred for the 25- and 50-Hz attenuation estimates.

An obvious result in Fig. 5 is the discrepancy among the top, bottom and top-and-bottom attenuation curves. We have only speculations for this surprising result which has been confirmed by repeated measurements and a variety of computations. Although the crushed limestone is assumed to be of the same technical specification and was obtained from the same retail source, it was delivered in two batches at an interval of one year. The first batch, which was used to fill the lower half of the tube, may have had higher moisture content than the second batch, which filled the top half of the tube. In porous materials, the addition of even a small amount of water content dramatically changes the acoustic properties of the material. For example, an increase in water content has been observed to increase the attenuation of acoustic waves in sand [21,22]. Gravitational compression or settling may be involved. Complicating matters is the fact that sound amplitude correlation measurements made at different heights in the tube did not result in significant variations of phase velocity with height, with the exception of estimates at 150 Hz, as discussed below. One conclusion that can be made is that in such a poorly defined medium as crushed limestone substantial variations in sound propagation parameters may occur.

4.1.1. Wavelength

Fig. 6 illustrates the variation of wavelength in crushed limestone with frequency, as determined by fitting the parameters of the standing wave function to the measured amplitude data both in the porous medium alone (porous medium fit) and in the entire tube (combined fit). Specifically, best-fit values of parameters of α_1, β_1, Γ_{01}, and A_0 were selected by searching for the values that minimized the mean squared difference between the measured rms sound pressures and Eq. (1). From the estimate of β_1, the corresponding estimate of wavelength was then calculated from $\lambda_1 = 2\pi/\beta_1$.

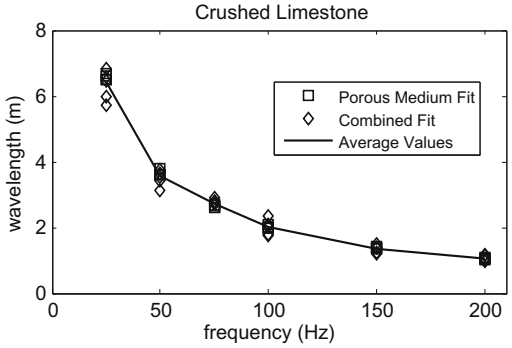

Fig. 6. Wavelength in crushed limestone. Data points are estimated from standing wave fits within the porous medium alone and from combined fits. The average curve is also indicated.

In this case the data appear to be well-conditioned to estimate wavelength from parameter fitting, as the results are consistent between the two fitting procedures. Efforts were also made to determine phase velocity from correlation of amplitudes from pairs of microphone ports (using the relationship between wavelength and phase velocity), with mixed results. While the wavelength values agreed at the higher frequencies, at 25 and 50 Hz the correlation-derived values exceed the parameter-fitted values by about 40%. This results from the difficulty experienced by the correlation method in the presence of high standing wave ratios. This is confirmed by computing the phase velocity from the wavelength data in Fig. 6 and plotting the result on Fig. 7. Each individual data point in these two figures derives from a separate application of the LMSE algorithm. The close agreement of the three phase velocity curves over most of the frequency range suggests that the two outlier points on the "bottom of tube" curve resulted from fortuitous convergence of their respective LMSE runs to false minima in parameter space.

The apparent variation of attenuation with depth prompted comparisons between phase velocities measured only in the bottom of the tube to those only in the top (all within the porous layer). The results are given in Fig. 7. While the data are noisy, it

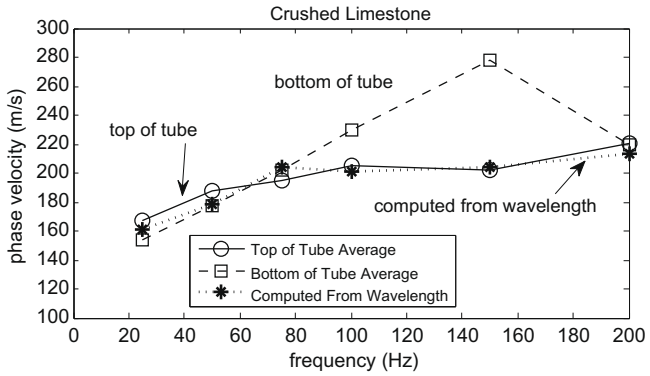

Fig. 7. Variation of phase velocity with frequency for crushed limestone. LMSE fits were performed separately for top and bottom halves of the porous layer [19]. The diamond-shaped data points were computed from the wavelengths in Fig. 6. The two outlier (square) points are believed to be erroneous.

appears that, with the exception of 150 Hz, the phase velocity did not vary significantly with depth. This is confirmed by computing the phase velocity from the wavelength data in Fig. 6 and plotting the result on Fig. 7. Each individual data point in these two figures derives from a separate application of the LMSE algorithm. The close agreement of the three phase velocity curves over most of the frequency range suggests that the two outlier points on the "bottom of tube" curve resulted from fortuitous convergence of their respective LMSE runs to false minima in parameter space.

4.1.2. Input impedance

The magnitude of the reflection coefficient $|\Gamma_{01}|$ and its phase Θ_{01} were obtained from fitting to Eq. (1). These results are shown in Table 1, for several frequencies and layer depths [19]. In Table 1, SWR is the pressure standing wave ratio in the air above the gravel column, and Z_{01}/Z_0 is the normalized input impedance. Input impedance is estimated by fitting the standing wave, including the reflection coefficient as a parameter, to the rms sound pressures in the air above the crushed limestone. Then, the input impedance is evaluated from $Z_{01} = Z_0(1+\Gamma_{01})/(1-\Gamma_{01})$, where $Z_0 = \omega\rho_0/\beta_0$ is the intrinsic impedance of air. The results vary strongly with frequency as the pressure-doubling termination of the tube results in high standing wave ratio at the lower frequencies.

Table 1
Crushed limestone standing wave parameters [20].

Freq	1 m				2 m			
	$\lvert\Gamma_{01}\rvert$	Θ_{01}	SWR	Z_{01}/Z_0	$\lvert\Gamma_{01}\rvert$	Θ_{01}	SWR	Z_{01}/Z_0
25	0.84	6.28	11.5	$11.5+0.0j$	0.47	4.65	2.77	$0.61-0.73j$
50	0.26	5.08	1.7	$1.18-0.56j$	0.73	3.58	6.41	$0.16-0.22j$
75	0.66	4.64	4.88	$0.29-0.64j$	0.52	2.2	3.17	$0.39+0.45j$
100	0.75	4.08	7	$0.18-0.50j$	0.67	0.5	5.06	$2.01+2.35j$
150	0.54	3.14	3.35	$0.30+0.0j$	0.58	3.83	3.6	$0.30-0.33j$
200	–	–	–	–	0.54	0.94	3.35	$1.08+1.33j$
	3 m				4 m			
25	0.69	4.15	5.45	$0.24-0.53j$	0.43	3.2	2.51	$0.40-0.03j$
50	0.59	1.7	3.88	$0.44+0.78j$	0.49	5.22	2.92	$0.99-1.12j$
75	0.59	5.65	3.88	$1.66-1.76j$	0.6	1.57	4	$0.47+0.88j$
100	0.6	3.33	4	$0.25-0.09j$	0.6	4.4	4	$0.37-0.66j$
150	0.65	4.65	4.71	$0.38-0.86j$	0.51	3.46	3.08	$0.33-0.14j$
200	0.56	6.22	3.55	$3.51-0.36j$	0.5	2.58	3	$0.36+0.26j$

$|\Gamma_{01}|$ is the reflection coefficient at the air/gravel boundary.
Θ_{01} is the phase angle of the reflection coefficient.
SWR is the standing wave ratio in the air.
Z_{01}/Z_0 is the ratio of the input impedance of the gravel to the intrinsic impedance of air.

4.2. Pea gravel

We performed standard sieve analysis (USACE 1970, ASTM 2007) with the following results: A poorly graded non-plastic fine gravel (USCS: GP, AASHTO: A-1-a). Approximately 65% of the particles were between 12.7 mm and 6.4 mm, 28% between 4.76 mm and 6.35 mm and the remaining 7% were smaller than 4.76 mm.

The pea gravel is somewhat more homogeneous in particle size and is smaller in comparison with the diameter of a microphone port than is the crushed limestone. It follows that there should be fewer local distortions of the sound pressure fields in the neighborhood of microphone ports, thus fewer anomalous pressure data

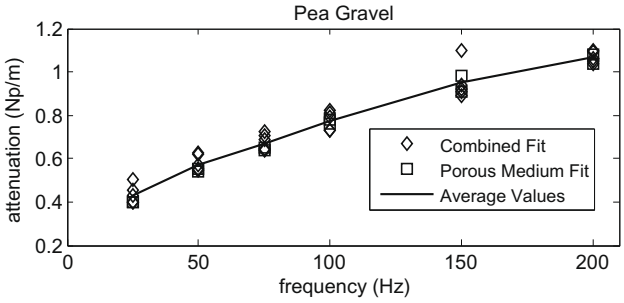

Fig. 8. Attenuation coefficient in pea gravel estimated by the combined fit and the porous medium fit.

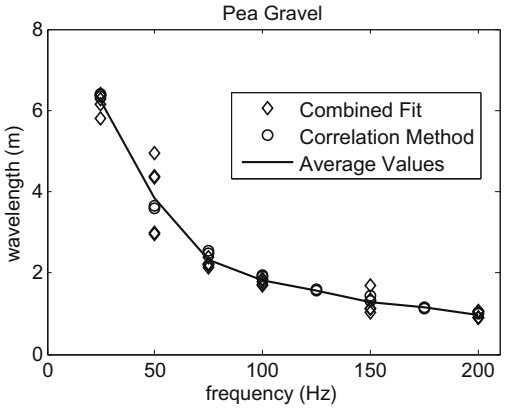

Fig. 9. Wavelength in pea gravel estimated by the combined fit and the correlation method. Due to high attenuation within the medium, the combined fit estimations have wide deviations at some frequencies. The correlation method proves to be very stable in the pea gravel since reflected waves are of low amplitude [19].

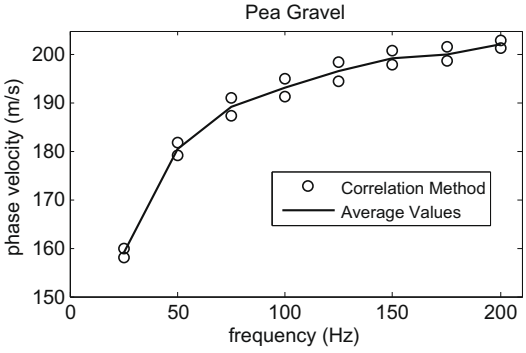

Fig. 10. Variation of phase velocity in pea gravel estimated by the correlation method.

Table 2
Pea gravel standing wave parameters [20]. Symbols as for Table 1.

Freq	1 m				2 m			
	$\lvert\Gamma_{01}\rvert$	Θ_{01}	SWR	Z_{01}/Z_0	$\lvert\Gamma_{01}\rvert$	Θ_{01}	SWR	Z_{01}/Z_0
25	0.86	6.28	13.46	13.451 – 0.32*j*	0.59	5.15	3.88	0.769 – 1.26*j*
50	0.58	6.09	3.73	3.339 – 1.091*j*	0.13	5.21	1.29	1.099 – 0.249*j*
75	0.59	5.31	3.90	0.947 – 1.43*j*	0.58	2.55	3.82	0.285 + 0.284*j*
100	0.70	5.08	5.70	0.511 – 1.32*j*	0.65	1.63	4.63	0.391 + 0.863*j*
150	0.69	4.79	5.47	0.381 – 1.004*j*	0.66	5.28	4.88	0.777 – 1.533*j*
200	0.52	3.97	3.21	0.365 – 0.389*j*	0.66	2.79	4.96	0.207 + 0.168*j*
	3 m				4 m			
25	0.76	4.08	7.33	0.171 – 0.495*j*	0.73	3.14	6.41	0.156 – 0.0*j*
50	0.65	1.70	4.63	0.369 + 0.809*j*	0.63	5.91	4.41	2.68 – 2.06*j*
75	0.61	5.65	4.13	1.616 – 1.858*j*	0.59	2.45	3.88	0.289 + 0.333*j*
100	0.62	3.46	4.25	0.241 – 0.149*j*	0.63	5.59	4.41	1.42 – 1.89*j*
150	0.48	5.18	2.87	0.963 – 1.082*j*	0.67	5.22	5.06	0.686 – 1.46*j*
200	0.43	0.03	2.50	2.494 + 0.082*j*	0.68	4.71	5.25	0.368 – 0.93*j*

points. Comparison of Fig. 5 with Fig. 8 suggests that the attenuation is higher in the pea gravel and that the standing waves are less pronounced owing to weaker reflected waves, especially near the top of the gravel column. It was judged that 4-m depth of pea gravel would suffice to characterize its wave propagation parameters, thus leaving a minimum of 3 m of air space to determine the input impedance of the gravel as terminated by the pressure-doubling plate.

4.2.1. Attenuation

Fig. 8 gives the attenuation vs. frequency for the pea gravel as determined by both the combined fit to both media at once and the fit in the porous medium alone. As the attenuation is relatively high, the porous medium fit procedure gives the more consistent results.

4.2.2. Wavelength

Fig. 9 gives the wavelength vs. frequency for pea gravel computed by both the combined fit and the correlation methods. As the attenuation in this medium is considerably greater than in the crushed limestone, the correlation method gives more repeatable results over three trials than does the combined fit method.

4.2.3. Phase velocity

Fig. 10 shows the phase velocity vs. frequency within the pea gravel. Again, due to the high attenuation, the correlation method provides the most consistent results. The pea gravel did not suffer from the same variations in phase velocity with depth that was observed in crushed limestone.

4.2.4. Input impedance

Standing wave parameters calculated in the air region of the pea gravel tests are reported in Table 2. Where there were multiple datasets for the same gravel depth, the complex reflection coefficients were averaged and the SWR and input impedance were calculated from those averages. These input impedances were estimated from fitting to the "air" portion of the tube in the same way as for the crushed limestone.

5. Comments

Gravels are poorly defined media, with acoustical parameters that can vary significantly from sample to sample. While the gravels used by the construction industry are classified in ways that are apparently adequate for the purposes of that industry, those classifications probably only loosely constrain the acoustical parameters. Thus, numerous repetitions of experimental tests of the sort presented here, in order to increase the precision of parameter estimation, are probably not justified. The results presented herein can be considered representative but not definitive with respect to construction classifications.

The initial approach to the measurement of acoustical parameters was to construct a Green's function representing an incident and a reflected wave of sound pressure in the tube, including both the gravel and the air above it, and to fit the parameters of the Green's function to the measured amplitudes by the minimization processes described earlier. In several cases, the combined fit proved unable to yield credible estimates for one or more parameters, perhaps because the measurement errors by chance affected those particular parameters excessively. Specifically, while the combined fit consistently yielded credible estimates of the wavelength and attenuation, estimates of the input impedance were very sensitive to small changes in the data. As an example, consider the estimated values of the acoustic parameters corresponding to Fig. 4 with best-fit values of 2.34 m, 0.49 Np/m, and 4.35 for the wavelength, attenuation coefficient and input impedance, respectively. If the data point corresponding to the microphone located at $z = 1.6$ m is removed, the LMSE remains the same but the best-fit parameters are 2.39 m, 0.47 Np/m, and 3.53 for the wavelength, attenuation coefficient and input impedance, respectively. This represents a change in the best-fit parameters of 2%, 4%, and 19% for the wavelength, attenuation coefficient and input impedance, respectively. While removal of one data point did not result in large changes in wavelength or attenuation estimates, significant changes were observed in the estimate of input impedance. Therefore, estimates of impedance appear to be very sensitive to measurement errors and less reliable. In those cases, restricting the fitting process to a smaller region of the tube sometimes yielded consistent results. In other cases, correlation methods or fitting to a simple real exponential function proved more reliable, especially when the reflected wave was substantially reduced by attenuation. In sum, for problems such as this, for which the measurements are inherently imprecise and in which several parameters are to be determined from the same data set, it may well be necessary to attack the problem in a piecemeal way, choosing methods which are optimal for specific parameters rather than attempting to estimate all parameters at once by the combined fit process.

Acknowledgments

This work was conducted under Agreement No. W9132T-06-2-0002, Upper Mississippi Valley Cooperative Ecosystems Studies Unit., between the University of Illinois at Urbana-Champaign

and the US Army Construction Engineering Research Laboratory (CERL). The experiments are conducted on the premises of and with the facilities of CERL. The authors acknowledge the contributions of former Graduate Research Assistants Timothy Onder, Ryan Lee, Timothy Eggerding and Todd Borrowman, and of CERL employees Dr. Larry Pater, Niels Svendsen, Dr. Michelle Swearingen, Jeffery Mifflin, Robert Klein and Bruce MacAllister. Thanks are given to two anonymous reviewers whose questions prompted significant revision of the manuscript.

References

[1] Attenborough K. Ground parameter information for propagation modeling. J Acoust Soc Am 1992;92:418–27. doi:10.1121/1.404251.
[2] Fellah ZEA, Fellah M, Sebaa N, Lauriks W, Depollier C. Measuring flow resistivity of porous materials at low frequencies range via acoustic transmitted waves (L). J Acoust Soc Am 2006;119:1926–8. doi:10.1121/1.2179749.
[3] Frederickson CK, Sabatier JM, Raspet R. Acoustic characterization of rigid-frame air-filled porous media using both reflection and transmission measurements. J Acoust Soc Am 1996;99:1326–32. doi:10.1121/1.414710.
[4] Horoshenkov KV, Hughes DC, Cwirzen A. The acoustic attenuation in porous cementitious materials. Appl Acoust 2003;64:197–212. doi:10.1016/S0003-682X(02)00069-5.
[5] Attenborough K. Acoustical impedance models for outdoor ground surfaces. J Sound Vib 1985;99:521–44. doi:10.1016/0022-460X(85)90538-3.
[6] Bolen LN, Bass HE. Effects of ground cover on the propagation of sound through the atmosphere. J Acoust Soc Am 1981;69:950–4. doi:10.1121/1.385618.
[7] Dickinson PJ, Doak PE. Measurements of the normal acoustic impedance of ground surfaces. J Sound Vib 1970;13:309–22. doi:10.1016/S0022-460X(70)80021-9.
[8] Embleton TFW, Piercy JE, Daigle GA. Effective flow resistivity of ground surfaces determined by acoustical measurements. J Acoust Soc Am 1983;74:1239–44. doi:10.1121/1.390029.
[9] Hess HM, Attenborough K, Heap NW. Ground characterization by short-range propagation measurements. J Acoust Soc Am 1990;87:1975–86. doi:10.1121/1.399325.
[10] Hickey CJ, Sabatier JM. Measurements of two types of dilatational waves in an air-filled unconsolidated sand. J Acoust Soc Am 1997;102:128–36. doi:10.1121/1.419770.
[11] Hutchinson-Howorth C, Attenborough K, Heap N. Indirect in situ and free-field measurement of impedance model parameters or surface impedance of porous layers. Appl Acoust 1993;39:77–117. doi:10.1016/0003-682X(93)90031-Z.
[12] Song BH, Bolton JS. A transfer-matrix approach for estimating the characteristic impedance and wave numbers of limp and rigid porous materials. J Acoust Soc Am 2000;107:1131–52. doi:10.1121/1.428404.
[13] Oelze ML, O'Brien Jr WD, Darmody RG. Measurement of attenuation and speed of sound in soil. Soil Sci Soc Am J 2002;66:788–96.
[14] Lu Z, Hickey CJ, Sabatier JM. Effects of compaction on the acoustic velocity in soils. Soil Sci Soc Am J 2004;68:7–16.
[15] Swenson Jr GW. A standing-wave facility for low-frequency impedance/absorption measurement. Appl Acoust 1993;40:355–62. doi:10.1016/0003-682X(93)90094-M.
[16] Lee J, Swenson Jr GW. Compact sound absorber for low frequencies. Noise Contr Eng J 1992;38:109–17. doi:10.3397/1.2827811.
[17] Swenson Jr GW, Onder TE, White MJ, Oelze ML. Estimating the acoustic properties of two kinds of gravel at frequencies between 25 and 200 Hz. US army CERL technical report ERDC/CERL SR-09-01; February 2009. <http://www.cecer.army.mil/techreports/ERDC-CERL_SR-09-1/ERDC-CERL_SR-09-1.pdf>.
[18] Weisstein EW. L2-norm, MathWorld—A wolfram web resource; July 2009. <http://mathworld.wolfram.com/L2-Norm.html>.
[19] Onder TE. Low-frequency sound wave behavior in porous media. MS thesis in electrical and computer engineering, University of Illinois at Urbana-Champaign; 2008.
[20] Eggerding TJ. Parameters of acoustic propagation through porous media. MS thesis in electrical and computer engineering, University of Illinois at Urbana-Champaign; 2008.
[21] Cramond AJ, Don CG. Effects of moisture content on soil impedance. J Acoust Soc Am 1987;82:293–301. doi:10.1121/1.395565.
[22] Horoshenkov KV, Mohamed MHA. Experimental investigation of the effects of water saturation on the acoustic admittance of sandy soils. J Acoust Soc Am 2006;120:1910–21. 10.1121:1.2338288.